



**HAL**  
open science

## The role of uncoupling protein 2 in macrophages and its impact on obesity-induced adipose tissue inflammation and insulin resistance

Xanthe A.M.H. van Dierendonck, Tiphaine Sancerni, Marie-Clotilde Alves-Guerra, Rinke Stienstra

### ► To cite this version:

Xanthe A.M.H. van Dierendonck, Tiphaine Sancerni, Marie-Clotilde Alves-Guerra, Rinke Stienstra. The role of uncoupling protein 2 in macrophages and its impact on obesity-induced adipose tissue inflammation and insulin resistance. *Journal of Biological Chemistry*, 2020, 295 (51), pp.17535-17548. 10.1074/jbc.RA120.014868 . hal-03418808

**HAL Id: hal-03418808**

**<https://hal.science/hal-03418808>**

Submitted on 10 Nov 2021

**HAL** is a multi-disciplinary open access archive for the deposit and dissemination of scientific research documents, whether they are published or not. The documents may come from teaching and research institutions in France or abroad, or from public or private research centers.

L'archive ouverte pluridisciplinaire **HAL**, est destinée au dépôt et à la diffusion de documents scientifiques de niveau recherche, publiés ou non, émanant des établissements d'enseignement et de recherche français ou étrangers, des laboratoires publics ou privés.

# The role of uncoupling protein 2 in macrophages and its impact on obesity-induced adipose tissue inflammation and insulin resistance

Received for publication, June 16, 2020, and in revised form, October 7, 2020. Published, Papers in Press, October 13, 2020, DOI 10.1074/jbc.RA120.014868

Xanthe A. M. H. van Dierendonck<sup>1,2</sup> , Tiphaine Sancerni<sup>3</sup>, Marie-Clotilde Alves-Guerra<sup>3</sup>, and Rinke Stienstra<sup>1,2,\*</sup>

From the <sup>1</sup>Nutrition, Metabolism, and Genomics Group, Division of Human Nutrition and Health, Wageningen University, Wageningen, The Netherlands, <sup>2</sup>Department of Internal Medicine, Radboud University Nijmegen Medical Centre, Nijmegen, The Netherlands, and <sup>3</sup>Université de Paris, Institut Cochin, INSERM, CNRS F-75014 Paris, France

Edited by Qi-Qun Tang

The development of a chronic, low-grade inflammation originating from adipose tissue in obese subjects is widely recognized to induce insulin resistance, leading to the development of type 2 diabetes. The adipose tissue microenvironment drives specific metabolic reprogramming of adipose tissue macrophages, contributing to the induction of tissue inflammation. Uncoupling protein 2 (UCP2), a mitochondrial anion carrier, is thought to separately modulate inflammatory and metabolic processes in macrophages and is up-regulated in macrophages in the context of obesity and diabetes. Here, we investigate the role of UCP2 in macrophage activation in the context of obesity-induced adipose tissue inflammation and insulin resistance. Using a myeloid-specific knockout of UCP2 (*Ucp2*<sup>ΔLysM</sup>), we found that UCP2 deficiency significantly increases glycolysis and oxidative respiration, both unstimulated and after inflammatory conditions. Strikingly, fatty acid loading abolished the metabolic differences between *Ucp2*<sup>ΔLysM</sup> macrophages and their floxed controls. Furthermore, *Ucp2*<sup>ΔLysM</sup> macrophages show attenuated pro-inflammatory responses toward Toll-like receptor-2 and -4 stimulation. To test the relevance of macrophage-specific *Ucp2* deletion *in vivo*, *Ucp2*<sup>ΔLysM</sup> and *Ucp2*<sup>fl/fl</sup> mice were rendered obese and insulin resistant through high-fat feeding. Although no differences in adipose tissue inflammation or insulin resistance was found between the two genotypes, adipose tissue macrophages isolated from diet-induced obese *Ucp2*<sup>ΔLysM</sup> mice showed decreased TNF $\alpha$  secretion after *ex vivo* lipopolysaccharide stimulation compared with their *Ucp2*<sup>fl/fl</sup> littermates. Together, these results demonstrate that although UCP2 regulates both metabolism and the inflammatory response of macrophages, its activity is not crucial in shaping macrophage activation in the adipose tissue during obesity-induced insulin resistance.

The occurrence of obesity and related metabolic disturbances, including insulin resistance and development of type 2 diabetes, has risen to epidemic proportions (1, 2). The chronic inflammatory processes that closely associate with a state of obesity are now widely recognized as important drivers of insulin resistance that may eventually evolve into type 2 diabetes (3). In particular the activation of macrophages in expanding

adipose tissue has been linked to this chronic, low-grade inflammation (3–7).

Dynamic changes in tissue microenvironments can drive specific metabolic alterations in tissue-resident immune cells in an attempt to accommodate appropriate changes in immune cell functioning (8). It is well known that modifications in metabolic signatures are closely related to immune cell functioning, demonstrated for instance by pro-inflammatory immune cells that rely on glycolytic pathways (9). Activation of macrophages in the context of obese adipose tissue was found to lead to unique changes in the metabolic signature of these adipose tissue macrophages (ATMs) (5, 7). This “metabolic activation” of macrophages was also linked to functional changes, such as the release of inflammatory cytokines (10). It is clear that modifications in metabolic signatures are crucial for appropriate immune cell functioning, yet might also drive immune cell dysfunction (11). Hence, specific metabolic reprogramming of adipose tissue macrophages driven by the lipid-enriched adipose tissue microenvironment during obesity might contribute to increased adipose tissue inflammation.

Uncoupling protein 2 (UCP2) is a mitochondrial carrier protein belonging to the SLC25 family of transporters (12). Although UCP2 mRNA is widely expressed throughout different tissues in mice, UCP2 protein can only be detected in spleen, lung, stomach, adipose tissue, and isolated immune cells, including macrophages (13–15). These findings underline the clear discrepancy between mRNA expression and protein expression (16). Potentially, the presence of UCP2 protein in immune cell-rich tissues such as spleen, lung, and adipose tissue could largely be attributable to the infiltration of immune cells. UCP2 shows a 59% homology to its family member uncoupling protein 1 (UCP1), known for robust uncoupling activity, although any uncoupling activity attributed to UCP2 is likely not physiological (12, 17–19). Nonetheless, in line with its presence in immune cells, UCP2 appears to play an important role in immune regulation, with UCP2 knockout mice showing increased survival after infections accompanied by an up-regulation in pro-inflammatory cytokines (20, 21).

UCP2 has been suggested to regulate metabolic pathways, determining the oxidation of glucose *versus* fatty acids in different cell types *in vitro* (22, 23) and in colorectal cancer cells *in vivo* (24). Possibly, UCP2 regulates cellular metabolism by being involved in the export of four-carbon substrates out of

This article contains supporting information.

\* For correspondence: Rinke Stienstra, rinke.stienstra@wur.nl.

This is an Open Access article under the CC BY license.

## UCP2 as regulator in adipose tissue macrophages

the mitochondria (25). In addition to its proposed metabolic role, several SNPs in *UCP2* were found to be related to obesity and type 2 diabetes (26–32).

Because of its involvement in both immune cell functioning and defining cellular metabolism of glucose *versus* fatty acids, UCP2 potentially provides an interesting target in elucidating the molecular mechanisms underlying immunometabolic reprogramming and activation of macrophages in the context of obesity-induced adipose tissue inflammation and insulin resistance. To investigate whether UCP2 plays a role in activation of adipose tissue macrophages, we first set out to determine the role of UCP2 in macrophages during inflammatory activation. Secondly, we evaluated the consequences of the absence of UCP2 in macrophages on the development of HFD-induced obesity and its complications including adipose tissue inflammation, glucose tolerance, and insulin resistance.

Our results reveal that UCP2 deficiency drives a distinct increase in glycolytic and oxidative metabolism in activated macrophages. Furthermore, specific *Ucp2* deletion attenuates pro-inflammatory activation in macrophages but does not alter the development of obesity-induced adipose tissue inflammation and insulin resistance.

### Results

#### Regulation of uncoupling protein 2 in macrophages during obesity and diabetes

We compared the regulation of UCP2 in three adipose tissue macrophage models: ATMs isolated from mice fed a high-fat diet (HFD) *versus* a low-fat diet (LFD) (10); bone marrow-derived macrophages (BMDMs) co-cultured with obese *versus* lean adipose tissue; and human adipose tissue macrophages isolated from obese diabetic patients *versus* obese nondiabetic patients (33) (Fig. 1A and Fig. S1). In all three macrophage-related models, *Ucp2* mRNA expression was up-regulated. Furthermore, after 10 to 16 weeks of HFD feeding in mice, *Ucp2* expression was increased in the adipose tissue (Fig. 1B). These levels likely correspond with the influx of immune cells into the adipose tissue, because increased *Ucp2* expression in the adipose tissue of HFD-fed *versus* LFD-fed (Ctrl) mice is mainly attributable to the stromal vascular fraction, including ATMs, and not to adipocytes (Fig. 1C). To be able to determine the role of UCP2 in regulating macrophage metabolism and activation in more detail, we generated mice with a myeloid-specific deletion of UCP2, using the Cre/loxP system coupled to the *Lys2* (*LysM*) promoter, resulting in *Ucp2*<sup>Δ*LysM*</sup> mice and their floxed control littermates (*Ucp2*<sup>fl/fl</sup>). The myeloid-specific deletion of UCP2 significantly silenced protein expression of UCP2 in BMDMs derived from *Ucp2*<sup>Δ*LysM*</sup> mice compared with *Ucp2*<sup>fl/fl</sup> control mice (Fig. 1D) and resulted in a nonsignificant trend toward decreased *Ucp2* mRNA expression in macrophage-rich tissues such as gonadal adipose tissue, spleen, and liver (Fig. 1E).

#### Deficiency of UCP2 increases glycolytic and oxidative metabolism in macrophages, which is attenuated by fatty acids

To understand the impact of UCP2 on cellular metabolism, we used extracellular flux assays. Basal glycolysis (Fig. 2A) and

maximal glycolytic capacity (Fig. 2B) were significantly increased in *Ucp2*<sup>Δ*LysM*</sup> *versus* *Ucp2*<sup>fl/fl</sup> macrophages, both during control conditions and during TLR4 agonist LPS-induced inflammation. Furthermore, relative mRNA expression of the glycolytic enzyme *Pfkfb3* was increased in *Ucp2*<sup>Δ*LysM*</sup> macrophages after LPS treatment, as was the production of lactate (Fig. S2, A and B). Basal (Fig. 2C) and maximal (Fig. 2D) respiration were significantly increased in *Ucp2*<sup>Δ*LysM*</sup> macrophages compared with *Ucp2*<sup>fl/fl</sup> cells during control conditions, and only basal respiration followed this pattern after LPS-induced inflammation. Strikingly, fatty acid loading abolished all differences observed in basal and maximal glycolysis (Fig. 2, E and F) and respiration (Fig. 2, G and H) between *Ucp2*<sup>Δ*LysM*</sup> and *Ucp2*<sup>fl/fl</sup> macrophages, in addition to abolishing differences in *Cpt1a* expression (Fig. S2C). Hence, UCP2 deficiency abolishes OA:PA-stimulated increases in glycolysis and maximal respiration.

#### Lack of UCP2 specifically attenuates macrophage response to inflammatory activation

Obesity-induced low-grade adipose tissue inflammation is linked to inflammatory activation of macrophages in adipose tissue with an important contribution of TLR2 and TLR4 receptor activation in driving metabolic inflammation (34). To study the role of UCP2 in macrophage activation, we tested the inflammatory response of *Ucp2*<sup>Δ*LysM*</sup> and *Ucp2*<sup>fl/fl</sup> macrophages toward TLR2 receptor agonist Pam3CysK (P3C) and TLR4 receptor agonist lipopolysaccharide (LPS) on both a transcriptional and a functional level (Fig. 3, A–E and Fig. 4, A–D). Treatment for 6 or 24 h with either LPS or P3C significantly increased the mRNA expression and protein secretion of all measured cytokines. Although most differences were relatively subtle, the pro-inflammatory response was generally attenuated in *Ucp2*<sup>Δ*LysM*</sup> *versus* *Ucp2*<sup>fl/fl</sup> macrophages treated with LPS, illustrated by lower *Il1b* expression after 24 h and lower *Il6* expression for both time points; *Tnfa* expression was not different (Fig. 4, A–C). For P3C, the differential effect was seen in *Il1b* expression for both time points. Accordingly, anti-inflammatory *Il10* expression was mostly up-regulated in *Ucp2*<sup>Δ*LysM*</sup> compared with *Ucp2*<sup>fl/fl</sup> macrophages, whereas *Il1ra* was clearly up-regulated after 6 h following LPS stimulation (Fig. 3D). On protein level, macrophage-specific deficiency of UCP2 generally subtly decreased the secretion of inflammatory cytokines IL6 and TNF $\alpha$  following LPS treatment while increasing IL10 secretion (Fig. 4, A–D).

#### Myeloid-specific UCP2 deficiency affects adipose tissue macrophage activation without affecting overall adipose tissue inflammation

Our next step was to test whether UCP2 in macrophages impacts adipose tissue inflammation and insulin resistance in an *in vivo* model of high-fat diet-induced obesity. *Ucp2*<sup>Δ*LysM*</sup> and their *Ucp2*<sup>fl/fl</sup> littermates were rendered obese and insulin resistant by being fed a high-fat diet for 16 weeks, using a low-fat diet as control. No differences between the two genotypes were found in body weight gain (Fig. 5A), feed intake (Fig. 5B), or adipose tissue and liver weights (Fig. 5C and Fig. S3).

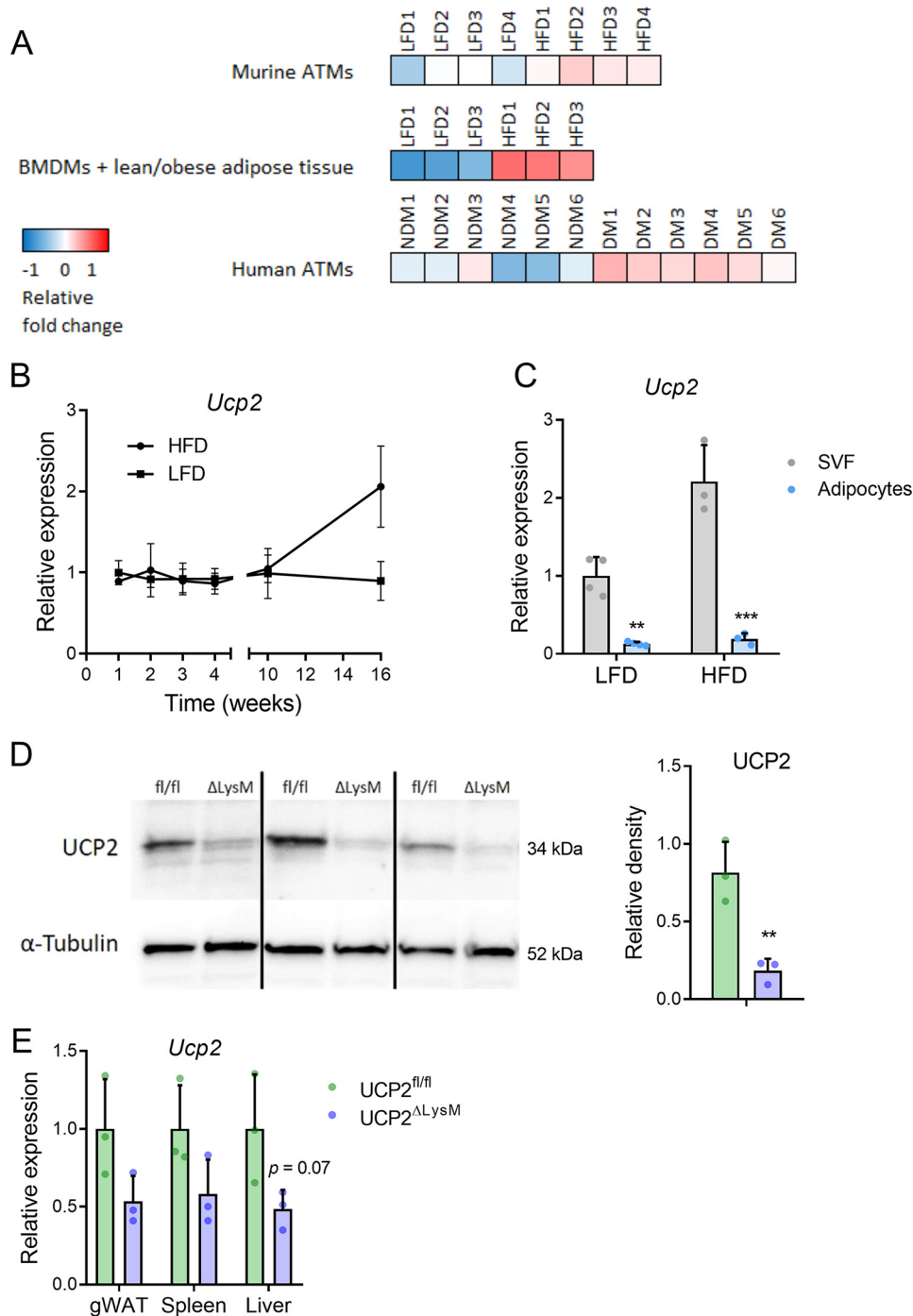


**Figure 1. Regulation of uncoupling protein 2 in macrophages during obesity and diabetes.** *A*, relative fold changes of *Ucp2* in adipose tissue macrophages isolated from lean and obese mice ( $n = 4$  mice per group); bone marrow-derived macrophages co-cultured with lean or obese adipose tissue explants ( $n = 3$  replicates per group) and CD14+ adipose tissue macrophages isolated from obese subjects with (DM) or without (NDM) diabetes type 2 ( $n = 6$  subjects per group). Per dataset, group means were significantly different ( $p < 0.05$ ,  $p < 0.01$ , and  $p < 0.05$ , respectively). *B*, relative expression of *Ucp2* in gonadal adipose tissue of C57Bl/6J mice fed a LFD or HFD for 1, 2, 3, 4, 10, and 16 weeks ( $n = 6$  per diet). *C*, relative expression of *Ucp2* in stromal vascular and adipocyte fractions of C57Bl/6J mice fed a LFD or HFD for 7 days ( $n = 3-4$ ). *D*, protein expression of UCP2 in *Ucp2<sup>fl/fl</sup>* and *Ucp2<sup>ΔLysM</sup>* bone-marrow derived macrophages. *E*, relative mRNA expression of *Ucp2* measured in gWAT, spleen, and liver of *Ucp2<sup>fl/fl</sup>* and *Ucp2<sup>ΔLysM</sup>* mice ( $n = 3$ ). Data are presented as mean  $\pm$  S.D. NDM, no diabetes mellitus; DM, diabetes mellitus; SVF, stromal vascular fraction. \*\*,  $p < 0.01$ ; \*\*\*,  $p < 0.001$ .

Additionally, plasma levels of triglycerides, nonesterified fatty acids, cholesterol, adiponectin, and leptin did not show any differences between *Ucp2<sup>ΔLysM</sup>* and *Ucp2<sup>fl/fl</sup>* mice (Fig. 5, *D* and *E*).

Subsequently, we isolated adipose tissue macrophages from the *Ucp2<sup>ΔLysM</sup>* and *Ucp2<sup>fl/fl</sup>* mice fed a high-fat diet. To com-

pare these to macrophages that did not reside in a lipid-rich microenvironment, we additionally isolated macrophages from the peritoneum of these mice and measured the release of inflammatory cytokines of both types of macrophages unstimulated, or upon an inflammatory stressor (LPS). In the *Ucp2<sup>ΔLysM</sup>* adipose tissue macrophages, no decrease was found

## UCP2 as regulator in adipose tissue macrophages

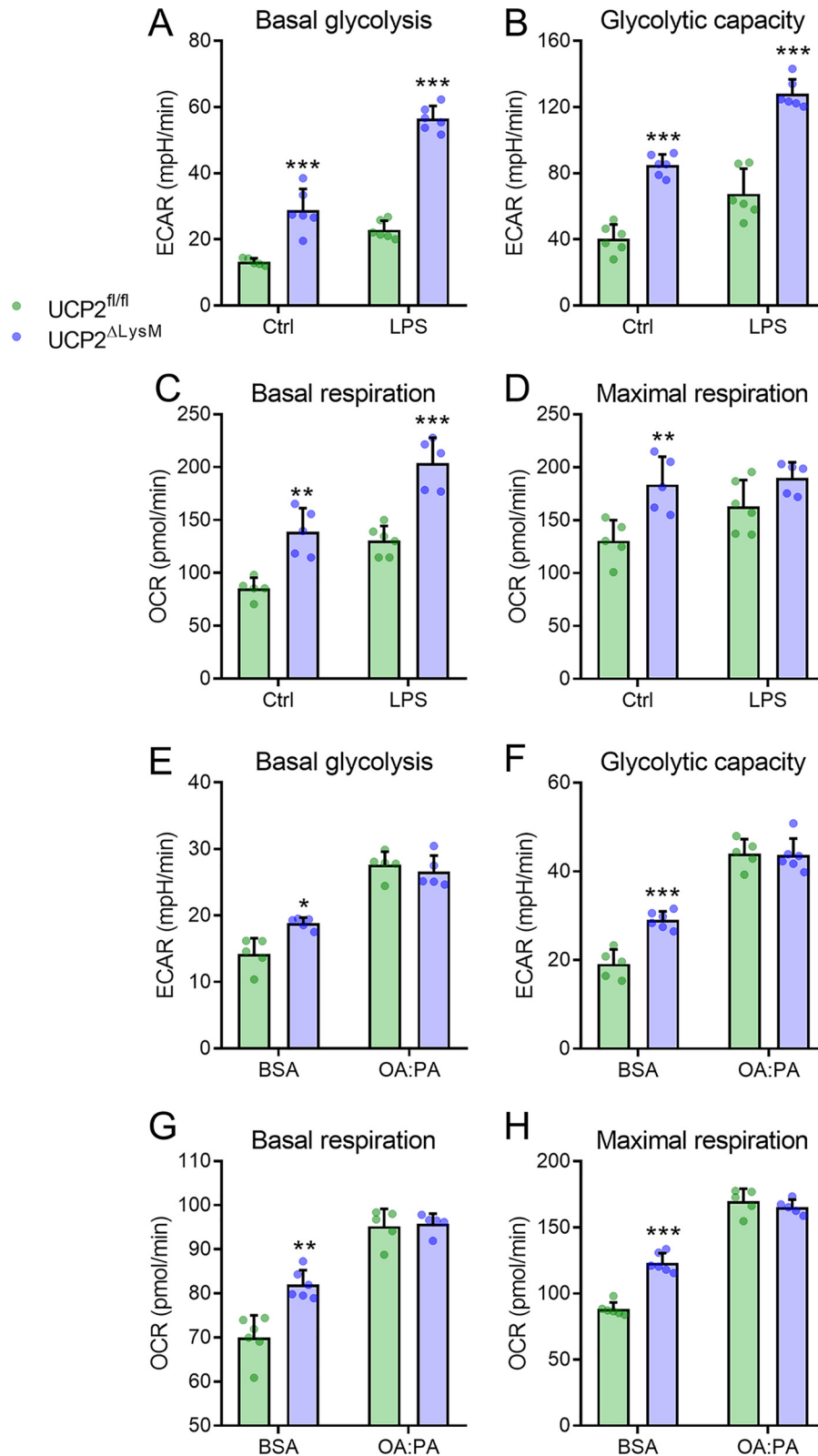


**Figure 2. Deficiency of UCP2 increases glycolytic and oxidative metabolism in macrophages; metabolic differences are attenuated by fatty acid influx.** A and B, basal glycolysis (A) and glycolytic capacity (B) based on extracellular acidification rates of *Ucp2<sup>fl/fl</sup>* and *Ucp2<sup>ΔLysM</sup>* BMDMs, treated with or without LPS for 24 h and subjected to glycolytic stress tests. C and D, basal (C) and maximal respiration (D) based on oxygen consumption rates of *Ucp2<sup>fl/fl</sup>* and *Ucp2<sup>ΔLysM</sup>* BMDMs, treated with or without LPS for 24 h and subjected to mitochondrial stress tests. E and F, basal glycolysis (E) and glycolytic capacity (F) based on extracellular acidification rates of *Ucp2<sup>fl/fl</sup>* and *Ucp2<sup>ΔLysM</sup>* BMDMs treated with oleate:palmitate conjugated to BSA or BSA alone for 24 h and subjected to glycolytic stress tests. G and H, basal (G) and maximal respiration (H) based on oxygen consumption rates of *Ucp2<sup>fl/fl</sup>* and *Ucp2<sup>ΔLysM</sup>* BMDMs treated with oleate:palmitate conjugated to BSA or BSA alone for 24 h and subjected to mitochondrial stress tests. Data presented as mean  $\pm$  S.D. for representative runs. ECAR, extracellular acidification rate; OCR, oxygen consumption rate; OA:PA, mixture of oleic acid and palmitic acid (2:1). \*,  $p < 0.05$ ; \*\*,  $p < 0.01$ ; \*\*\*,  $p < 0.001$ .

● UCP2<sup>fl/fl</sup>  
● UCP2<sup>ΔLysM</sup>

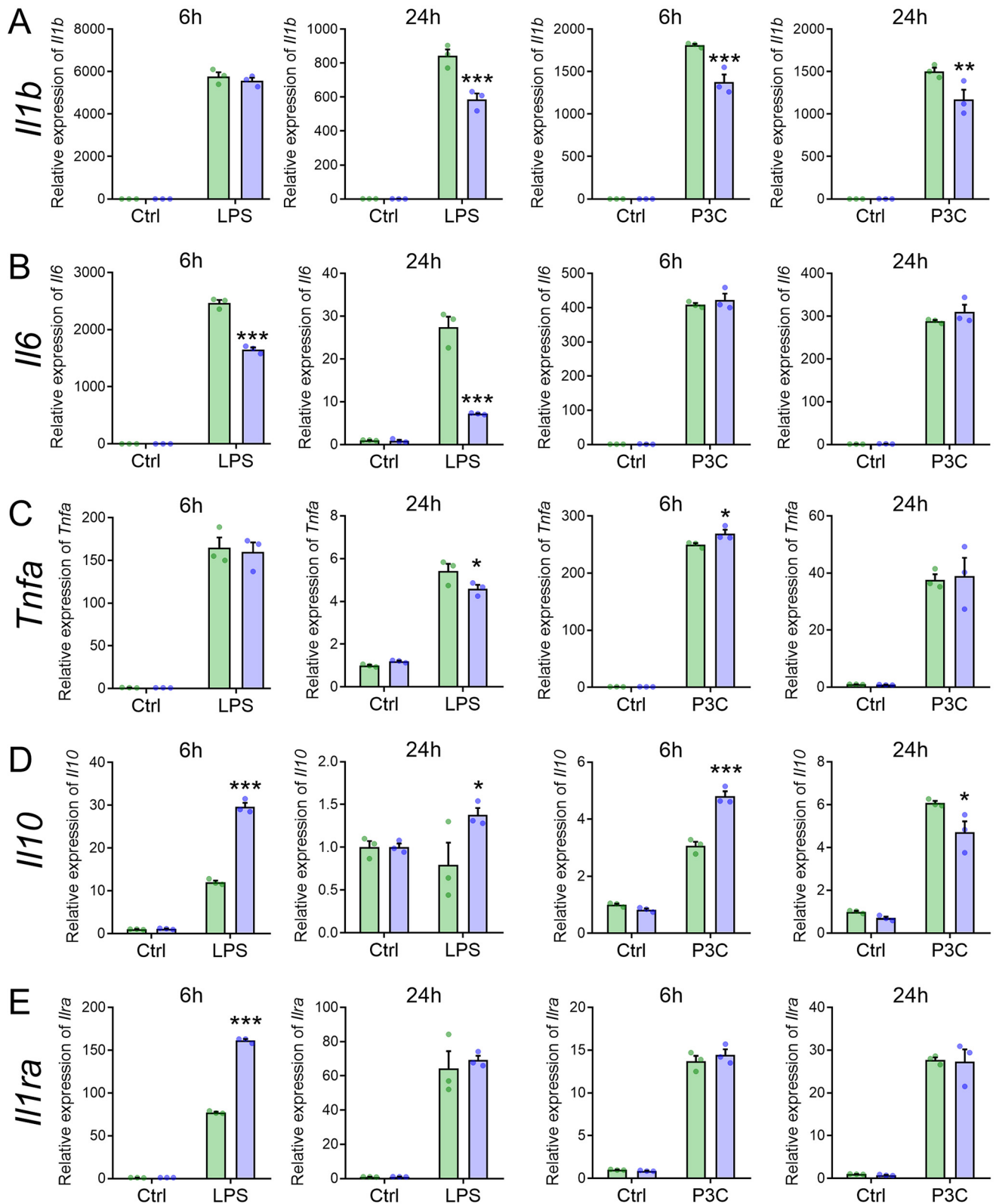


**Figure 3. Lack of UCP2 specifically attenuates transcriptional pro-inflammatory activation of macrophages.** A–E, relative expression of *Il1b* (A), *Il6* (B), *Tnfa* (C), *Il10* (D), and *Il1ra* (E) in *Ucp2*<sup>fl/fl</sup> and *Ucp2*<sup>ΔLysM</sup> BMDMs treated with 10 ng/ml LPS or 5 μg/ml P3C for 6 or 24 h. Data are presented as mean ± S.D. P3C, Pam3CysK. \*, *p* < 0.05; \*\*\*, *p* < 0.001.

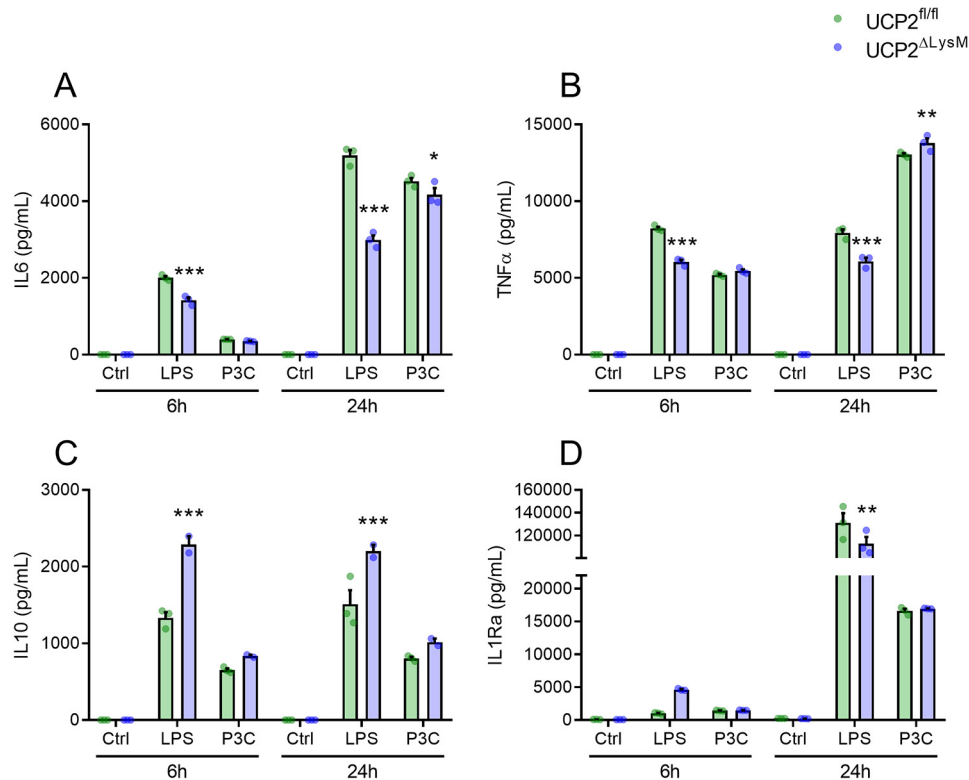


**Figure 4. Lack of UCP2 modulates cytokine secretion toward a less pro-inflammatory phenotype in macrophages.** A–D, production of IL6 (A), TNF $\alpha$  (B), IL10 (C), and IL1Ra (D) in *Ucp2*<sup>fl/fl</sup> and *Ucp2*<sup>ΔLysM</sup> BMDMs treated with 10 ng/ml LPS or 5  $\mu$ g/ml P3C for 6 or 24 h. Data are presented as mean  $\pm$  S.D. P3C, Pam3-CysK. \*,  $p < 0.05$ ; \*\*,  $p < 0.01$ ; \*\*\*,  $p < 0.001$ .

in IL6 (Fig. 6A), but a significant decrease was found in the levels of TNF $\alpha$  (Fig. 6B) and IL1Ra (Fig. 6D), and a similar trend for IL10 (Fig. 6C) after LPS stimulation. In contrast, both IL6 and TNF $\alpha$  levels remained unchanged in peritoneal macrophages isolated from *Ucp2*<sup>ΔLysM</sup> versus *Ucp2*<sup>fl/fl</sup> mice after *ex vivo* LPS stimulation (Fig. 6, E and F).

Next, we assessed inflammation of total adipose tissue. Flow cytometry of the stromal vascular fraction derived from gonadal adipose tissue (gWAT) of obese *Ucp2*<sup>ΔLysM</sup> and *Ucp2*<sup>fl/fl</sup> mice revealed that there was no relative difference in general (F4/80+) or pro-inflammatory (F4/80+CD11c+) macrophage populations between the two genotypes (Fig. 7A). Additionally, relative mRNA expression of macrophage markers *Cd68* and *Adgre1* (F4/90) did not differ significantly (Fig. 7B). Moreover, mRNA expression of cytokines involved in the inflammatory response of adipose tissue (*Il1b*, *Tnfa*, *Il6*, and *Il10*) was not found to be significantly altered between the genotypes (Fig. 7C), as was the release of IL6 and IL10 (Fig. 7D). The density of crownlike structures stained for macrophage marker F4/80 did not differ between obese adipose tissue from *Ucp2*<sup>ΔLysM</sup> versus their *Ucp2*<sup>fl/fl</sup> littermates (Fig. 7E and F). Also, no differences were found in the mRNA expression of inflammatory markers in the liver, nor any differences in liver histology (Fig. S4, A–C). On a systemic level, we found no significant differences in either insulin tolerance (Fig. 8, A and B) or glucose tolerance (Fig. 8, C and D) in *Ucp2*<sup>ΔLysM</sup> and *Ucp2*<sup>fl/fl</sup> mice. Furthermore, nonfasted levels of both insulin and glucose did not differ significantly between the two genotypes after either low-fat or high-fat diet feeding (Fig. 8, E and F).

## Discussion

This is the first study determining the function of UCP2 in macrophages during low-grade adipose tissue inflammation in the context of obesity and type 2 diabetes. Here, we demonstrate that lack of UCP2 leads to an up-regulation of both glycolytic and oxidative metabolism in macrophages, which is overruled after an influx of lipids. Furthermore, UCP2-deficiency specifically attenuates the macrophage response to inflammation, without impacting overall adipose tissue inflammation or systemic glucose homeostasis.

The expression of UCP2 protein is not linked to mRNA expression levels because of translational regulation of UCP2 (16). In this study, we use a macrophage-specific deletion of UCP2 that was confirmed by using a highly specific, nonambiguous UCP2 antibody (13), which enables us to study UCP2 while minimizing the induction of nonphysiological changes.

The results of our research confirm the immunomodulatory role that was previously attributed to UCP2. We were able to show that lack of UCP2 leads to general attenuation of the pro-inflammatory response of macrophages toward LPS and P3C *in vitro*. Additionally, *Ucp2*<sup>ΔLysM</sup> adipose tissue macrophages isolated from obese adipose tissue displayed an overall blunted response to LPS treatment *ex vivo*, with decreased TNF $\alpha$  and IL1Ra levels. Interestingly, in earlier studies, loss of *Ucp2* was shown to promote inflammation, translating into prolonging survival of mice in infection models (20, 21). However, these models used whole-body *Ucp2*<sup>-/-</sup> mice, which still leaves macrophage-specific roles unclear. Furthermore, the enhancement of inflammation by *Ucp2* knockout is often attributed to

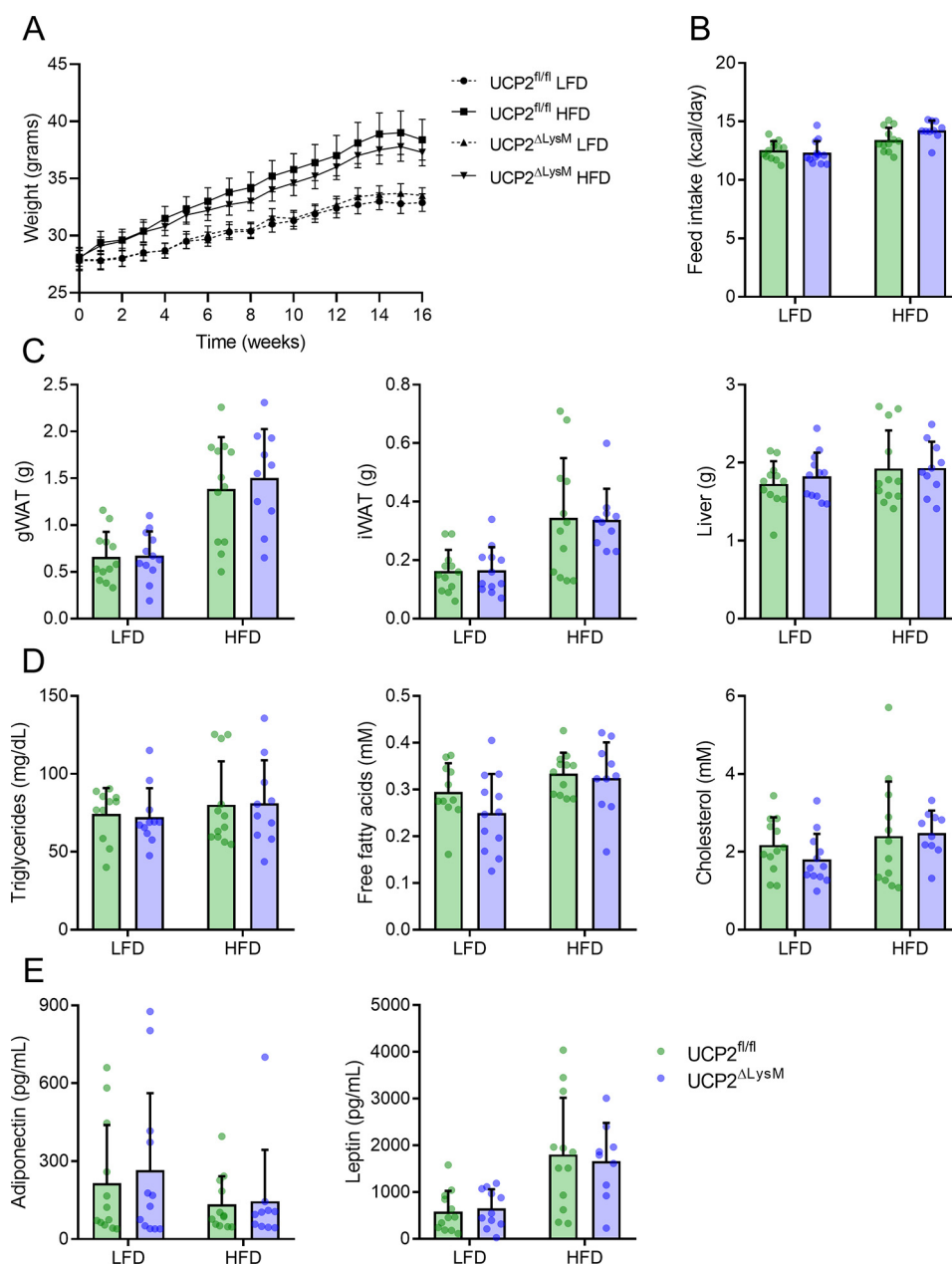


**Figure 5. Macrophage-specific UCP2 deletion does not lead to general differences in LFD- or HFD-fed mice.** A–E, body weight (A); feed intake (B); gWAT, iWAT, and liver weight (C); plasma concentrations of triglycerides, free fatty acids, and cholesterol (D); adiponectin and leptin (E) of *Ucp2<sup>fl/fl</sup>* and *Ucp2<sup>ΔLysM</sup>* mice ( $n = 24$  *Ucp2<sup>fl/fl</sup>* and 22 *Ucp2<sup>ΔLysM</sup>*) fed either LFD or HFD for 16 weeks. Data are presented as mean  $\pm$  S.D. or mean  $\pm$  S.E. (A). iWAT, inguinal white adipose tissue.

increased ROS production, although the induction of ROS in *Ucp2<sup>-/-</sup>* cells is not always present or consistent (23). Particularly macrophage-specific *Ucp2<sup>-/-</sup>* models have led to inconsistent results related to ROS induction (35, 36), leading to contradictory results related to the contribution of UCP2 in modulating inflammatory responses specifically in macrophages. A more recent study showed that enhanced survival of *Ucp2<sup>-/-</sup>* mice in a model of sepsis was coupled to a decreased inflammatory phenotype (37). In their study, Moon and colleagues (37) suggest that macrophage-specific loss of UCP2 leads to reduced inflammasome activation through inhibition of fatty acid synthase signaling, resulting in lower inflammatory activation. Together with these findings, our results underline

the importance of UCP2 in linking metabolic signatures and inflammatory output in macrophages. Hereby, UCP2-deficient macrophages are less equipped to successfully adapt to inflammatory environments and subsequently demonstrate an attenuated inflammatory response.

UCP2 was previously identified as a protein that can regulate cellular metabolism by exporting four-carbon substrates, favoring oxidative respiration (22, 23, 25, 35). Loss of UCP2 had earlier been found to lead to metabolic shifts in glucose utilization (24) and to limit metabolic flexibility in resting macrophages because of incomplete oxidation (38). Accordingly, in UCP2-deficient macrophages we observed an increased glycolytic rate, both in resting, nontreated cells as well as after LPS

## UCP2 as regulator in adipose tissue macrophages

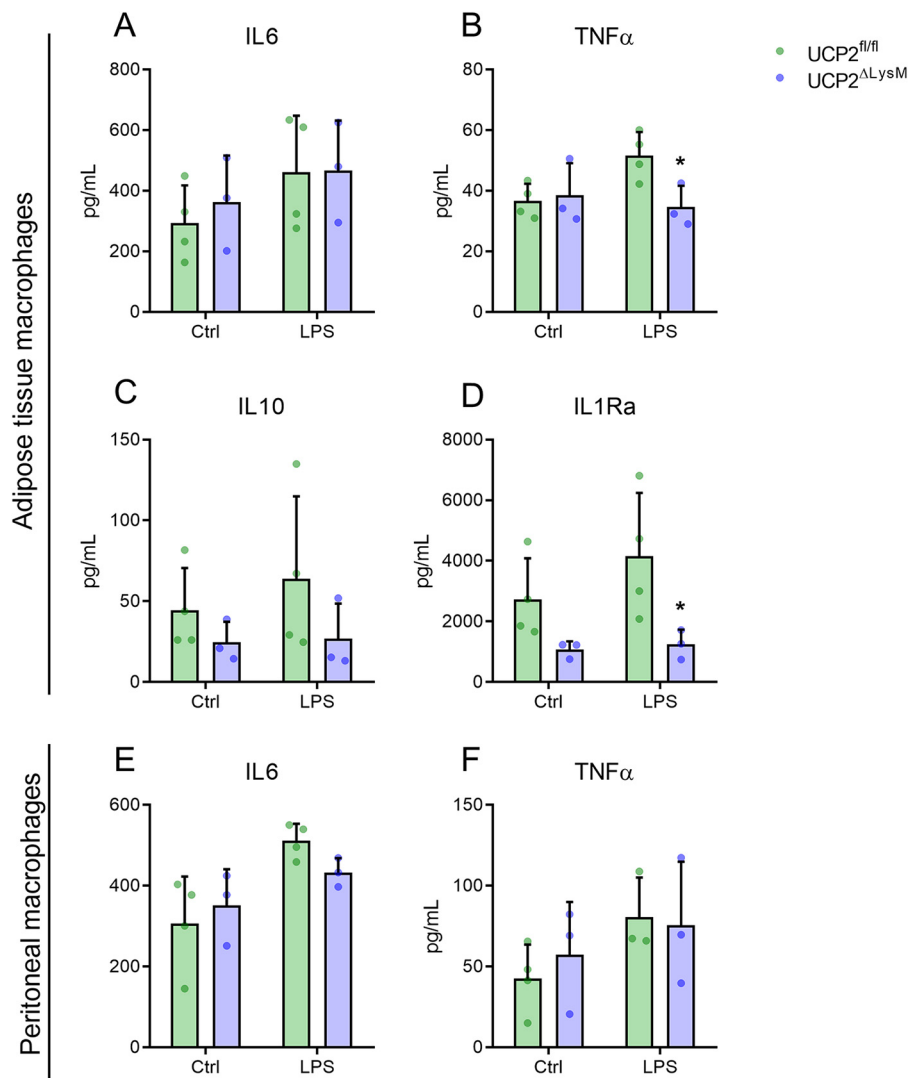


**Figure 6. UCP2 deficiency impacts cytokine secretion in adipose tissue macrophages, but not peritoneal macrophages in HFD-fed mice.** A–F, production of IL6 (A), TNF $\alpha$  (B), IL1ra (C), and IL10 (D) in adipose tissue macrophages and IL6 (E) and TNF $\alpha$  (F) in peritoneal macrophages isolated from  $Ucp2^{fl/fl}$  and  $Ucp2^{\Delta LysM}$  mice fed a HFD for 16 weeks and treated with LPS or vehicle (Ctrl) for 24 h. Data are normalized to DNA concentrations per well and are presented as mean  $\pm$  S.D. \*,  $p < 0.05$ .

treatment. Although increased glycolytic flux is seen as a key characteristic for inflammatory macrophages (39),  $Ucp2^{\Delta LysM}$  macrophages actually display an attenuated pro-inflammatory response after treatment. In these macrophages, enforced metabolic inflexibility likely disconnects metabolic rewiring from inflammatory activation, exemplified by the impaired adaptation to inflammatory environments.

Interestingly, after exposure to fatty acids, relevant for macrophages residing in adipose tissue, differences in glycolytic and oxidative metabolism between  $Ucp2^{\Delta LysM}$  and  $Ucp2^{fl/fl}$  macrophages disappear. This finding is in accordance with data from Xu *et al.* (35), who found no difference in fatty acid-induced  $\beta$ -oxidation between UCP2-deficient and control macrophages after lipid loading. The abolishment of metabolic differences after fatty acid loading suggests that changes in immune cell metabolism are uncoupled from the presence or activation of UCP2 during the influx of lipids. Therefore, although UCP2 seems an important component in determining effective metabolic adaptation during basal or inflammatory

states, it is not a crucial component in controlling macrophage metabolism in the presence of high amounts of lipids. Instead, after knockdown of UCP2, the cell is able to bypass the UCP2-driven mechanism and relies on other mechanisms to deal with the increased influx of fatty acids. Likely, these lipids activate the nuclear receptor PPAR $\gamma$ , which controls the expression of numerous lipid-related genes in macrophages (40) next to regulating *Ucp2* (41).

Based on our *in vitro* studies, we hypothesized that UCP2 deficiency in adipose tissue macrophages might attenuate inflammatory activation, leading to a decrease in adipose tissue inflammation in obese  $Ucp2^{\Delta LysM}$  mice. The blunted inflammatory response of  $Ucp2^{\Delta LysM}$  versus  $Ucp2^{fl/fl}$  adipose tissue macrophages after *ex vivo* stimulation with LPS is in line with our hypothesis. However, no evidence of decreased adipose tissue inflammation nor reduced glucose tolerance was found *in vivo*. Several explanations may exist as to why loss of UCP2 in macrophages does not impact on inflammation of the adipose tissue or glucose tolerance upon HFD-induced obesity. Although

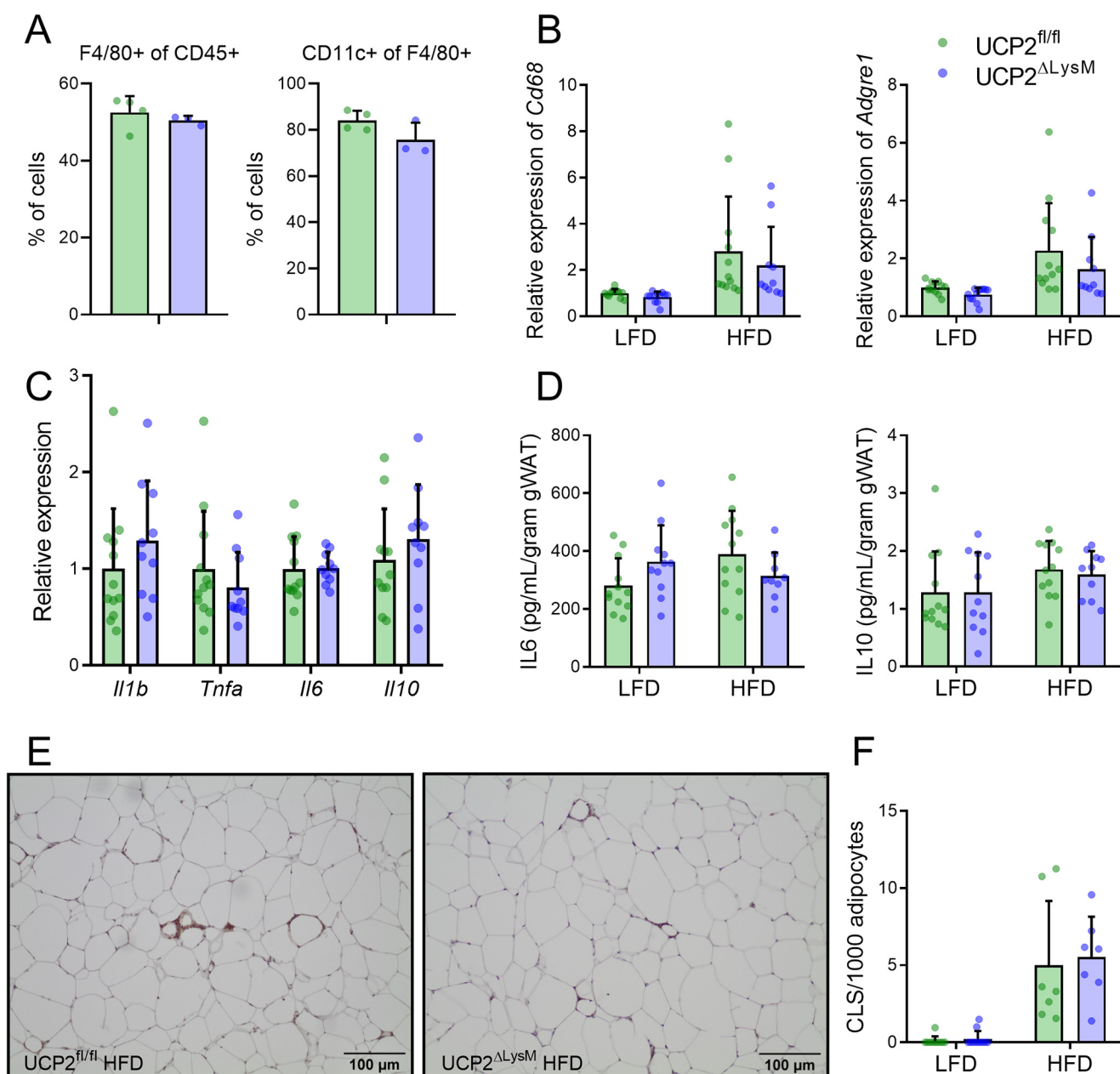


**Figure 7. Macrophage-specific UCP2 deletion does not impact adipose tissue inflammation after HFD feeding.** A, flow cytometry analysis of CD45+F4/80+ cells and CD45+F4/80+CD11c+ cells in the stromal vascular fractions isolated from  $Ucp2^{fl/fl}$  and  $Ucp2^{\Delta LysM}$  mice fed a HFD for 16 weeks. Relative mRNA expression of immune cell markers *Cd68* and *Adgre1* B–D, relative expression of inflammatory cytokines *Il1b*, *Tnfa*, *Il6*, and *Il10* (C, only for HFD) and production of IL6 and IL10 in gWAT from  $Ucp2^{fl/fl}$  and  $Ucp2^{\Delta LysM}$  mice fed either a LFD or a HFD for 16 weeks (D). E and F, density of crownlike structures (CLS) in gWAT F4/80 stained coupes from  $Ucp2^{fl/fl}$  and  $Ucp2^{\Delta LysM}$  mice fed a HFD for 16 weeks. Scale bar represents 100  $\mu$ m. Data are presented as mean  $\pm$  S.D.

the blunted response of adipose tissue macrophages hints toward a difference in inflammatory phenotype between  $Ucp2^{\Delta LysM}$  and  $Ucp2^{fl/fl}$  macrophages, this phenotype only became apparent after *ex vivo* stimulation with LPS. Because UCP2 seems to be a more subtle regulator of cellular metabolism (24), which is dispensable for most metabolic processes in the absence of constraints (12), substantial stressors are needed to uncover the consequences of UCP2 deletion. Hence, the inflammatory factors present in obese adipose tissue that lead to metabolic activation of adipose tissue macrophages (42) might not be potent enough to lead to a phenotype similar to

activation by LPS. Next to that, as seen *in vitro*, the presence of high amounts of lipids leads to an unaltered metabolic status in both  $Ucp2^{\Delta LysM}$  and  $Ucp2^{fl/fl}$  macrophages, likely similar to the *in vivo* situation in the adipose tissue. These observations together could serve to explain the lack of differences in adipose tissue inflammation between  $Ucp2^{\Delta LysM}$  and  $Ucp2^{fl/fl}$  mice.

Several potential limitations existed in this study. Because functional UCP2 antibody is scarce and UCP2 protein expression is not directly linked to mRNA expression, detailed mechanistic studies are complicated. Furthermore, because

## UCP2 as regulator in adipose tissue macrophages

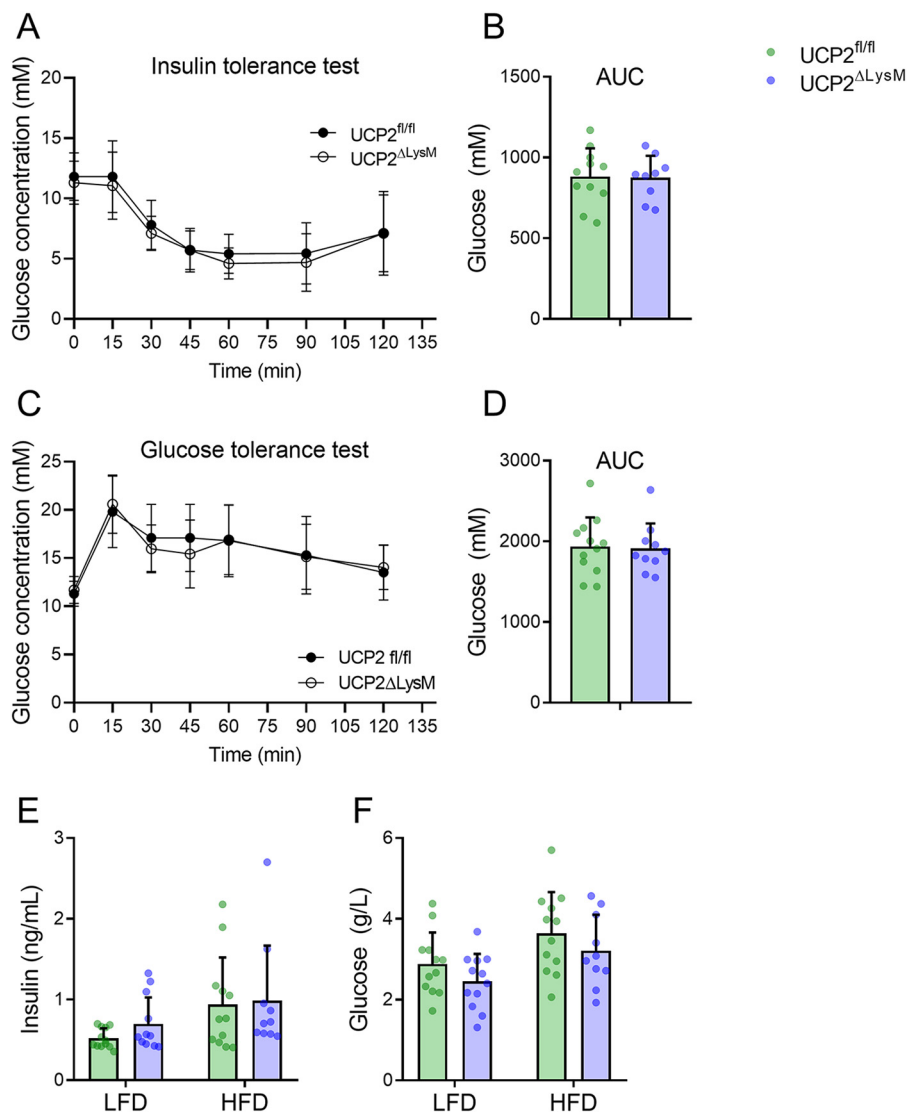


**Figure 8. UCP2 deletion in macrophages does not impact systemic insulin or glucose tolerance.** A–D, intraperitoneal insulin tolerance test (A and B) and oral glucose tolerance test (C and D) of *Ucp2<sup>fl/fl</sup>* and *Ucp2<sup>ΔLysM</sup>* mice fed an HFD for 16 weeks. E and F, nonfasted insulin (E) and glucose (F) levels in plasma of *Ucp2<sup>fl/fl</sup>* and *Ucp2<sup>ΔLysM</sup>* mice fed either LFD or HFD for 16 weeks. Data presented as mean ± S.D. AUC, area under the curve.

the *Ucp2<sup>ΔLysM</sup>* model is myeloid-specific in the whole organism, any potential differences in the *in vivo* phenotype could have been attributable to deletion of UCP2 in myeloid cells in other organs, including the brain (43). Lastly, only male mice were used for the *in vivo* studies, possibly leading to bias.

In conclusion, UCP2 has a role in modulating both metabolism and inflammatory response in macrophages. When UCP2 is specifically deleted in macrophages, both glycolytic and oxidative metabolism are up-regulated, although metabolic differences equalize after fatty acid loading. Furthermore, UCP2 deficiency in macrophages attenuates the pro-inflammatory response toward LPS, also in adipose tissue macrophages, but does not impact adipose tissue inflammation after high-fat feeding. Therefore, although UCP2 modulates macrophage metabolism and subsequent inflammatory responses, its presence is not essential to shape ATM activation during lipid influx or obesity.

## Experimental procedures

### Animal studies

For the animal studies, purebred WT C57BL/6J animals (The Jackson Laboratory, Bar Harbor, ME), *Ucp2<sup>ΔLysM</sup>* mice and their floxed littermates, were used. UCP2<sup>fl/fl</sup> mice were acquired from The Jackson Laboratory (B6;129S-Ucp2tm2.1Lowl/J; Bar Harbor, ME) and crossed at least five generations with C57BL/6J mice. Subsequently, UCP2<sup>fl/fl</sup> mice were crossed with lysM-Cre transgenic mice (The Jackson Laboratory, Bar Harbor, ME; B6.129P2-Lyz2tm1 (cre)Ifo/J, no. 004781) to generate mice with a specific Cre-mediated deletion of UCP2 in the mature myeloid cell fraction. Mice were housed individually under normal light–dark cycles in temperature- and humidity-controlled specific pathogen-free conditions. Mice had *ad libitum* access to food and water. All animal experiments were carried out in accordance with the EU Directive 2010/63/EU for animal experiments.

To induce obesity and insulin resistance, male *Ucp2*<sup>ΔLysM</sup> mice age 9–12 weeks and their male floxed littermates were placed on a high-fat diet for 16 weeks. To calculate the power, previous data on fasting glucose values were used. Fasting glucose values of mice fed a high-fat diet may differ on average 3 mM ( $\pm$  8–11 mM) compared with mice fed a low-fat diet. Differences in responses might lead to an S.D. around 2 mM or higher. To perform the power calculation, we used a one-way analysis of variance with a significance level of 0.05 and a power of 90%, leading to an estimation of around  $n = 11$  mice needed per group. To allow for the compensation of unforeseen circumstances or potential loss of mice during the study,  $n = 12$  mice were included per group. Thus, 12 mice per genotype were randomly allocated to a standardized high-fat diet or a low-fat diet for 16 weeks (D12451 and D12450H, Research Diets, New Brunswick, NJ, USA;  $\gamma$ -irradiated with 10–20 kilograys).

Body weight and food intake were assessed weekly. At the end of the study, mice were anesthetized with isoflurane and blood was collected via orbital puncture in tubes containing EDTA (Sarstedt, Nümbrecht, Germany). Subsequently, mice were immediately euthanized by cervical dislocation, after which tissues were excised, weighed, and frozen in liquid nitrogen or prepared for histology. Samples from liquid nitrogen were stored at  $-80^{\circ}\text{C}$ . All animal experiments were approved by the local animal welfare committee of Wageningen University (2016.W-0093.002). The experimenter was blinded to group assignments during all analyses.

#### **Intraperitoneal glucose and insulin tolerance test**

Glucose and insulin tolerance tests were performed after 14 or 15 weeks by oral gavage of glucose (0.8 g/kg, Baxter) or intraperitoneal injection of insulin (0.75 units/kg, Novo Nordisk). Mice were fasted for 5 h prior to the tolerance tests and blood was collected at 0, 15, 30, 45, 60, 90, and 120 min after administration of glucose or insulin by tail bleeding. Blood glucose was measured using glucose sensor strips and a GLUCOFIX Tech glucometer (GLUCOFIX Tech, Menarini Diagnostics, Valkenswaard, the Netherlands).

#### **Plasma measurements**

Blood collected in EDTA tubes was spun down for 15 min at 5000 rpm and at  $4^{\circ}\text{C}$ . Plasma was aliquoted and stored at  $-80^{\circ}\text{C}$ . Measurement of insulin (Ultra Sensitive Mouse Insulin ELISA Kit, Crystal Chem USA, Elk Grove Village, IL, USA), glucose (Liquicolor, Human GmbH, Wiesbaden, Germany), adiponectin (Adiponectin ELISA DuoSet Kit, R&D Systems), leptin (Leptin ELISA DuoSet Kit, R&D Systems), cholesterol (Liquicolor), triglycerides (Liquicolor), and nonesterified fatty acids (NEFA-HR set R1, R2 and standard, WAKO Diagnostics, InstruChemie, Delfzijl, the Netherlands).

#### **Explants and isolation of adipose tissue macrophages**

After collection of gonadal adipose tissue (gWAT), part of the gWAT was separated and transferred on ice in Dulbecco's modified Eagle's medium (DMEM, Corning, NY, USA), supplemented with 1% penicillin/streptomycin (p/s) (Corning), and 1% FFA-free BSA (BSA fraction V, Roche via Merck). For each

mouse, an explant of 50 mg was kept in culture for 24 h in DMEM supplemented with 10% FCS (BioWest, Nuaille, France) and 1% p/s, after which supernatant was collected for ELISA measurements or harvested as conditioned medium. Stromal vascular fractions of gWAT was isolated by collagenase digestion for 45 min in RPMI 1630 medium (Lonza, Basel, Switzerland) supplemented with 10% FCS, 1% p/s, 0.5% FFA-free BSA, 1 M  $\text{CaCl}_2$ , 1 M HEPES, and 0.15% collagenase (from *Clostridium histolyticum*, Merck). gWAT was pooled for three mice of the same group after digestion, mature adipocytes were stored separately, and erythrocytes were lysed with ACK buffer. From the resulting stromal vascular cells, 500,000 cells were sampled for flow cytometry; remaining cells were used for ATM isolation. ATMs were isolated by magnetic separation using the OctoMACS Cell Separator System with MS columns, mouse anti-F4/80-FITC antibody, and anti-FITC MicroBeads (all Miltenyi Biotec, Bergisch Gladbach, Germany). ATMs were kept in culture in RPMI 1630 with 10% FCS and 1% p/s for 24 h in the presence or absence of 10 ng/ml LPS (Merck) to obtain supernatants.

#### **Flow cytometry**

Stromal vascular cells were stained with antibodies against CD45-ECD (Beckman Coulter), F4/80-FITC, CD206-APC, CD11c-PE-Cy7, and CD11b-PE (BioLegend, San Diego, CA, USA). Samples were measured on a flow cytometer (FC500, Beckman Coulter) and results were analyzed using Kaluza analysis software 2.1 (Beckman Coulter).

#### **Histological studies**

gWAT and liver samples were fixed in 3.7% paraformaldehyde and embedded in paraffin. Sectioned slides were stained with hematoxylin and eosin according to standard protocols. Sections were incubated 20% normal goat serum before overnight incubation with F4/80 antibody (MCA497G, Bio-Rad). Secondary antibodies used were anti-rat or anti-rabbit IgG conjugated to HRP (Cell Signaling Technology, Danvers, MA, USA). No primary antibody was used for negative controls.

#### **Primary cell isolation**

Peritoneal macrophages were harvested from the mice by injection washing the peritoneal cavity with ice-cold PBS and F4/80 based magnetic separation was used to ensure purity (see isolation ATMs). Peritoneal macrophages were kept in culture for 24 h in RPMI 1630 with 10% FCS and 1% p/s with or without the presence of 10 ng/ml LPS (Merck) to obtain supernatants. For BMDM isolation, 8- to 12-week-old *Ucp2*<sup>ΔLysM</sup> and their *Ucp2*<sup>fl/fl</sup> littermates were euthanized by cervical dislocation. Femurs were isolated, bone marrow was extracted and differentiated in DMEM, supplemented with 10% FCS, 1% p/s and 15% L929 conditioned medium. After 7 days of differentiation, BMDMs were scraped and plated as appropriate.

#### **Cell culture experiments**

Palmitate (Merck) and oleate (Merck) were solubilized using EtOH and KOH and conjugated to FFA-free BSA in sterile water (Versol, Aguetant, Lyon, France) at  $37^{\circ}\text{C}$  for 30 min.

## UCP2 as regulator in adipose tissue macrophages

Oleate was used at a concentration of 200  $\mu\text{M}$  or a mixture of oleate and palmitate (oleate:palmitate) was made in a ratio of 2:1 and used in a final concentration of 600  $\mu\text{M}$ . BSA was used as control for fatty acid treatments. LPS (Merck) was used in a concentration of 10 ng/ml, P3C (Merck) was used in a concentration of 5  $\mu\text{g/ml}$ , both were diluted in PBS. All cells were washed with PBS (Corning) before treatment. For macrophage-adipose tissue co-cultures (Fig. 1A), BMDMs were plated in 12-well plates and after adhesion, an insert was added with 100 mg of carefully minced live adipose tissue isolated from mice fed a HFD or LFD for 13–16 weeks. BMDMs were co-cultured with adipose tissue for 24 h.

### Extracellular flux assay

To measure extracellular flux in BMDMs, the Agilent Seahorse XF96 Analyzer (Agilent Technologies, Santa Clara, CA, USA) was used. Cells were seeded in XF-96 plates (Agilent Technologies) in a density of 200,000 cells/well, and treated with LPS or fatty acids appropriately. Before flux measurement, cells were washed and cultured for an hour in Seahorse XF base medium (Agilent Technologies) at 37°C in a non-CO<sub>2</sub> incubator until the measurement. The base medium was set to a pH of 7.4 and was supplemented with 2 mM L-glutamine for glycolytic stress tests or 2 mM L-glutamine and 25 mM glucose for mitochondrial stress tests. Glycolytic stress tests included the injection of glucose (25 mM) after which basal glycolysis was measured, oligomycin (1.5  $\mu\text{M}$ ) after which glycolytic capacity was measured and 2-deoxyglucose (50 mM). Mitochondrial stress tests included the injection of oligomycin (1.5  $\mu\text{M}$ ), carbonyl cyanide *p*-trifluoromethoxyphenylhydrazone (FCCP) (1.5  $\mu\text{M}$ ), plus pyruvate (1 mM) after which maximal respiration was measured, and antimycin A (2.5  $\mu\text{M}$ ) plus rotenone (1.25  $\mu\text{M}$ ). Basal respiration was measured unstimulated. All experiments were performed at least with quadruplicates. Oxygen consumption rate and extracellular acidification rate were measured at baseline, and following the injections, calculations were made using Wave Desktop 2.6 (Agilent Technologies).

### Real-time PCR and microarray

For cells and liver tissue, total RNA was isolated using TRIzol<sup>®</sup> Reagent (Invitrogen, Thermo Fisher Scientific). For gWAT, total RNA was isolated with the RNeasy Micro Kit (Qiagen, Venlo, the Netherlands). The iScript cDNA kit was used to synthesize cDNA (Bio-Rad) according to manufacturer's instructions. The CFX384 Touch<sup>™</sup> Real-Time Detection System (Bio-Rad) was used to perform real time PCR, using a SensiMix<sup>™</sup> (BioLine, London, UK) based protocol. Human *B2M* and mouse *36b4* expression were used to normalize values for human and mouse samples, respectively. The microarray datasets used for Fig. 1A were described earlier (10, 33).

### Immunoblotting

Cell protein lysates were separated by electrophoresis on a precast 4–20% Tris-glycine gel (SDS-PAGE) (Bio-Rad) and transferred onto nitrocellulose membranes using a liquid transfer cell (all purchased from Bio-Rad), blocked in nonfat milk and incubated overnight at 4°C with primary antibody and sub-

sequently for 1 h with appropriate peroxidase conjugate antibody at room temperature. Membranes were developed with the chemiluminescence substrate (SuperSignal West Pico PLUS, Thermo Fisher Scientific) and images were captured with the ChemiDoc MP system (Bio-Rad). The primary antibodies for UCP2 were described earlier (13). Full membranes are shown in Figure S5.

### ELISA

TNF $\alpha$ , IL10, IL1ra, and IL6 levels were measured in cell or explant supernatant with DuoSet sandwich ELISA kits for (R&D Systems) according to manufacturer's instructions. To normalize the data, the concentration of DNA per well was measured for adipose tissue macrophages and peritoneal macrophages (Quant-iT dsDNA Assay Kit High Sensitivity, Thermo Fisher Scientific). For gWAT explants, the exact weight per explant was used for normalization.

### Lactate assay

Proteins were removed from cell supernatants using perchloric acid precipitation to avoid contamination with lactate dehydrogenase. Lactate concentrations were determined using conversion of lactate by lactate oxidase (Merck), and subsequent oxidation of Amplex Red reagent (Thermo Fisher Scientific) into resorufin by HRP (Thermo Fisher Scientific), which was measured as a fluorescent signal.

### Data and statistical analysis

Data are represented as mean  $\pm$  S.D. as indicated in the legend. Statistical analyses were carried out using the unpaired Student's *t* test or two-way analysis of variance followed by Bonferroni's post hoc multiple comparisons test, if genotype and diet or genotype and treatment were both found significant (GraphPad Software, San Diego, CA, USA). A value of  $p < 0.05$  was considered statistically significant.

### Data availability

All data are contained within the manuscript. Microarray datasets that were used were described earlier (10, 33).

---

*Acknowledgments*—We thank Shohreh Keshtkar, Jenny Jansen, Desiree Vorstenbosch, Julia van Heck, and Anneke Hijmans for technical assistance.

*Author contributions*—X. A. M. H. v. D. and R. S. conceptualization; X. A. M. H. v. D. data curation; X. A. M. H. v. D. formal analysis; X. A. M. H. v. D. validation; X. A. M. H. v. D. investigation; X. A. M. H. v. D. visualization; X. A. M. H. v. D. and T. S. methodology; X. A. M. H. v. D. writing-original draft; X. A. M. H. v. D. and R. S. project administration; X. A. M. H. v. D., T. S., M.-C. A.-G., and R. S. writing-review and editing; T. S. and M.-C. A.-G. resources; R. S. supervision; R. S. funding acquisition.

*Funding and additional information*—This work was supported by Vidi Grant from the NWO and by Dutch Diabetes Foundation senior fellowship 2015.82.1824 (to R. S.).

**Conflict of interest**—The authors declare that they have no conflicts of interest with the contents of this article.

**Abbreviations**—The abbreviations used are: ATM, adipose tissue macrophage; gWAT, gonadal white adipose tissue; HFD, high-fat diet; LFD, low-fat diet; BMDM, bone marrow-derived macrophages; Ctrl, control; LPS, lipopolysaccharide; OA:PA, mixture of oleic acid and palmitic acid; p/s, penicillin/streptomycin.

## References

- NCD Risk Factor Collaboration. (2016) Trends in adult body-mass index in 200 countries from 1975 to 2014: A pooled analysis of 1698 population-based measurement studies with 19.2 million participants. *Lancet* **387**, 1377–1396 [CrossRef Medline](#)
- Cornier, M.-A., Després, J.-P., Davis, N., Grossniklaus, D. A., Klein, S., Lamarche, B., Lopez-Jimenez, F., Rao, G., St-Onge, M.-P., Towfighi, A., and Poirier, P. (2011) Assessing adiposity: A scientific statement from the American Heart Association. *Circulation* **124**, 1996–2019 [CrossRef Medline](#)
- Odegaard, J. I., and Chawla, A. (2008) Mechanisms of macrophage activation in obesity-induced insulin resistance. *Nat. Clin. Pract. Endocrinol. Metab.* **4**, 619–626 [CrossRef Medline](#)
- Weisberg, S. P., McCann, D., Desai, M., Rosenbaum, M., Leibel, R. L., and Ferrante, A. W. (2003) Obesity is associated with macrophage accumulation in adipose tissue. *J. Clin. Invest.* **112**, 1796–1808 [CrossRef Medline](#)
- Xu, X., Grijalva, A., Skowronski, A., van Eijk, M., Serlie, M. J., and Ferrante, A. W. (2013) Obesity activates a program of lysosomal-dependent lipid metabolism in adipose tissue macrophages independently of classic activation. *Cell Metab.* **18**, 816–830 [CrossRef Medline](#)
- Cinti, S., Mitchell, G., Barbatelli, G., Murano, I., Ceresi, E., Faloia, E., Wang, S., Fortier, M., Greenberg, A. S., and Obin, M. S. (2005) Adipocyte death defines macrophage localization and function in adipose tissue of obese mice and humans. *J. Lipid Res.* **46**, 2347–2355 [CrossRef Medline](#)
- Kratz, M., Coats, B. R., Hisert, K. B., Hagman, D., Mutskov, V., Peris, E., Schoenfelt, K. Q., Kuzma, J. N., Larson, I., Billing, P. S., Landerholm, R. W., Crouthamel, M., Gozal, D., Hwang, S., Singh, P. K., et al. (2014) Metabolic dysfunction drives a mechanistically distinct proinflammatory phenotype in adipose tissue macrophages. *Cell Metab.* **20**, 614–625 [CrossRef Medline](#)
- Loftus, R. M., and Finlay, D. K. (2016) Immunometabolism: Cellular metabolism turns immune regulator. *J. Biol. Chem.* **291**, 1–10 [CrossRef Medline](#)
- Lachmandas, E., Boutens, L., Ratter, J. M., Hijmans, A., Hooiveld, G. J., Joosten, L. A. B., Rodenburg, R. J., Fransen, J. A. M., Houtkooper, R. H., van Crevel, R., Netea, M. G., and Stienstra, R. (2016) Microbial stimulation of different Toll-like receptor signalling pathways induces diverse metabolic programmes in human monocytes. *Nat. Microbiol.* **2**, 16246 [CrossRef Medline](#)
- Boutens, L., Hooiveld, G. J., Dhingra, S., Cramer, R. A., Netea, M. G., and Stienstra, R. (2018) Unique metabolic activation of adipose tissue macrophages in obesity promotes inflammatory responses. *Diabetologia* **61**, 942–953 [CrossRef Medline](#)
- O'Neill, L. A. J., Kishton, R. J., and Rathmell, J. (2016) A guide to immunometabolism for immunologists. *Nat. Rev. Immunol.* **16**, 553–565 [CrossRef Medline](#)
- Bouillaud, F., Alves-Guerra, M.-C., and Ricquier, D. (2016) UCPs, at the interface between bioenergetics and metabolism. *Biochim. Biophys. Acta* **1863**, 2443–2456 [CrossRef Medline](#)
- Pecqueur, C., Alves-Guerra, M. C., Gelly, C., Levi-Meyrueis, C., Couplan, E., Collins, S., Ricquier, D., Bouillaud, F., and Miroux, B. (2001) Uncoupling protein 2, in vivo distribution, induction upon oxidative stress, and evidence for translational regulation. *J. Biol. Chem.* **276**, 8705–8712 [CrossRef Medline](#)
- Alves-Guerra, M.-C., Rousset, S., Pecqueur, C., Mallat, Z., Blanc, J., Tedgui, A., Bouillaud, F., Cassard-Doulcier, A.-M., Ricquier, D., and Miroux, B. (2003) Bone marrow transplantation reveals the *in vivo* expression of the mitochondrial uncoupling protein 2 in immune and nonimmune cells during inflammation. *J. Biol. Chem.* **278**, 42307–42312 [CrossRef Medline](#)
- Mattiasson, G., and Sullivan, P. G. (2006) The emerging functions of UCP2 in health, disease, and therapeutics. *Antioxid. Redox Signal.* **8**, 1–38 [CrossRef Medline](#)
- Hurtaud, C., Gelly, C., Bouillaud, F., and Lévi-Meyrueis, C. (2006) Translational control of UCP2 synthesis by the upstream open reading frame. *Cell. Mol. Life Sci.* **63**, 1780–1789 [CrossRef Medline](#)
- Bouillaud, F. (2009) UCP2, not a physiologically relevant uncoupler but a glucose sparing switch impacting ROS production and glucose sensing. *Biochim. Biophys. Acta* **1787**, 377–383 [CrossRef Medline](#)
- Couplan, E., del Mar Gonzalez-Barroso, M., Alves-Guerra, M. C., Ricquier, D., Gubern, M., and Bouillaud, F. (2002) No evidence for a basal, retinoic, or superoxide-induced uncoupling activity of the uncoupling protein 2 present in spleen or lung mitochondria. *J. Biol. Chem.* **277**, 26268–26275 [CrossRef Medline](#)
- Li, N., Karaca, M., and Maechler, P. (2017) Upregulation of UCP2 in beta-cells confers partial protection against both oxidative stress and glucotoxicity. *Redox Biol.* **13**, 541–549 [CrossRef Medline](#)
- Arsenijevic, D., Onuma, H., Pecqueur, C., Raimbault, S., Manning, B. S., Miroux, B., Couplan, E., Alves-Guerra, M.-C., Gubern, M., Surwit, R., Bouillaud, F., Richard, D., Collins, S., and Ricquier, D. (2000) Disruption of the uncoupling protein-2 gene in mice reveals a role in immunity and reactive oxygen species production. *Nat. Genet.* **26**, 435–439 [CrossRef Medline](#)
- Rousset, S., Emre, Y., Join-Lambert, O., Hurtaud, C., Ricquier, D., and Cassard-Doulcier, A.-M. (2006) The uncoupling protein 2 modulates the cytokine balance in innate immunity. *Cytokine* **35**, 135–142 [CrossRef Medline](#)
- Esteves, P., Pecqueur, C., Ransy, C., Esnous, C., Lenoir, V., Bouillaud, F., Bulteau, A. L., Lombès, A., Prip-Buus, C., Ricquier, D., and Alves-Guerra, M. C. (2014) Mitochondrial retrograde signaling mediated by UCP2 inhibits cancer cell proliferation and tumorigenesis. *Cancer Res.* **74**, 3971–3982 [CrossRef Medline](#)
- Pecqueur, C., Bui, T., Gelly, C., Hauchard, J., Barbot, C., Bouillaud, F., Ricquier, D., Miroux, B., and Thompson, C. B. (2008) Uncoupling protein-2 controls proliferation by promoting fatty acid oxidation and limiting glycolysis-derived pyruvate utilization. *FASEB J.* **22**, 9–18 [CrossRef Medline](#)
- Aguilar, E., Esteves, P., Sancerni, T., Lenoir, V., Aparicio, T., Bouillaud, F., Dentin, R., Prip-Buus, C., Ricquier, D., Pecqueur, C., Guilmeau, S., and Alves-Guerra, M. C. (2019) UCP2 deficiency increases colon tumorigenesis by promoting lipid synthesis and depleting NADPH for antioxidant defenses. *Cell Rep.* **28**, 2306–2316.e5 [CrossRef Medline](#)
- Voza, A., Parisi, G., De Leonardis, F., Lasorsa, F. M., Castegna, A., Amorse, D., Marmo, R., Calcagnile, V. M., Palmieri, L., Ricquier, D., Paradies, E., Scarcia, P., Palmieri, F., Bouillaud, F., and Fiermonte, G. (2014) UCP2 transports C4 metabolites out of mitochondria, regulating glucose and glutamine oxidation. *Proc. Natl. Acad. Sci.* **111**, 960–965 [CrossRef Medline](#)
- Oktavianthi, S., Trimarsanto, H., Febinia, C. A., Suastika, K., Saraswati, M. R., Dwipayana, P., Arindrarto, W., Sudoyo, H., and Malik, S. G. (2012) Uncoupling protein 2 gene polymorphisms are associated with obesity. *Cardiovasc. Diabetol.* **11**, 41 [CrossRef Medline](#)
- Martinez-Hervas, S., Mansego, M. L., de Marco, G., Martinez, F., Alonso, M. P., Morcillo, S., Rojo-Martinez, G., Real, J. T., Ascaso, J. F., Redon, J., Martin Escudero, J. C., Soriguer, F., and Chaves, F. J. (2012) Polymorphisms of the UCP2 gene are associated with body fat distribution and risk of abdominal obesity in Spanish population. *Eur. J. Clin. Invest.* **42**, 171–178 [CrossRef Medline](#)
- Meyer, T. E., Boerwinkle, E., Morrison, A. C., Volcik, K. A., Sanderson, M., Coker, A. L., Pankow, J. S., and Folsom, A. R. (2010) Diabetes genes and prostate cancer in the atherosclerosis risk in communities study. *Cancer Epidemiol. Biomarkers Prev.* **19**, 558–565 [CrossRef Medline](#)
- Salopuro, T., Pulkkinen, L., Lindström, J., Kolehmainen, M., Tolppanen, A.-M., Eriksson, J. G., Valle, T. T., Aunola, S., Ilanne-Parikka, P., Keinänen-Kiukkaanniemi, S., Tuomilehto, J., Laakso, M., and Uusitupa, M. (2009) Variation in the UCP2 and UCP3 genes associates with abdominal

## UCP2 as regulator in adipose tissue macrophages

- obesity and serum lipids: The Finnish Diabetes Prevention Study. *BMC Med. Genet.* **10**, 94 [CrossRef Medline](#)
30. Andersen, G., Dalgaard, L. T., Justesen, J. M., Anthonen, S., Nielsen, T., Thørnø, L. W., Witte, D., Jørgensen, T., Clausen, J. O., Lauritzen, T., Holmkvist, J., Hansen, T., and Pedersen, O. (2013) The frequent *UCP2* -866G>A polymorphism protects against insulin resistance and is associated with obesity: A study of obesity and related metabolic traits among 17,636 Danes. *Int. J. Obes.* **37**, 175–181 [CrossRef Medline](#)
  31. Lyssenko, V., Almgren, P., Anevski, D., Orho-Melander, M., Sjögren, M., Saloranta, C., Tuomi, T., Groop, L., and Botnia Study Group. (2005) Genetic prediction of future type 2 diabetes. *PLoS Med.* **2**, e345 [CrossRef Medline](#)
  32. Esterbauer, H., Schneitler, C., Oberkofler, H., Ebenbichler, C., Paulweber, B., Sandhofer, F., Ladurner, G., Hell, E., Strosberg, A. D., Patsch, J. R., Krempler, F., and Patsch, W. (2001) A common polymorphism in the promoter of *UCP2* is associated with decreased risk of obesity in middle-aged humans. *Nat. Genet.* **28**, 178–183 [CrossRef Medline](#)
  33. Dalmas, E., Venteclaf, N., Caer, C., Poitou, C., Cremer, I., Aron-Wisniewsky, J., Lacroix-Desmazes, S., Bayry, J., Kaveri, S. V., Clément, K., André, S., and Guerre-Millo, M. (2014) T cell-derived IL-22 amplifies IL-1 $\beta$ -driven inflammation in human adipose tissue: Relevance to obesity and type 2 diabetes. *Diabetes* **63**, 1966–1977 [CrossRef Medline](#)
  34. Könnner, A. C., and Brüning, J. C. (2011) Toll-like receptors: linking inflammation to metabolism. *Trends Endocrinol. Metab.* **22**, 16–23 [CrossRef Medline](#)
  35. Xu, H., Hertzel, A. V., Steen, K. A., Wang, Q., Suttles, J., and Bernlohr, D. A. (2015) Uncoupling lipid metabolism from inflammation through fatty acid binding protein-dependent expression of *UCP2*. *Mol. Cell Biol.* **35**, 1055–1065 [CrossRef Medline](#)
  36. Emre, Y., and Nübel, T. (2010) Uncoupling protein *UCP2*: When mitochondrial activity meets immunity. *FEBS Lett.* **584**, 1437–1442 [CrossRef Medline](#)
  37. Moon, J.-S., Lee, S., Park, M.-A., Siempos, I. I., Haslip, M., Lee, P. J., Yun, M., Kim, C. K., Howrylak, J., Ryter, S. W., Nakahira, K., and Choi, A. M. K. (2015) *UCP2*-induced fatty acid synthase promotes NLRP3 inflammasome activation during sepsis. *J. Clin. Invest.* **125**, 665–680 [CrossRef Medline](#)
  38. Nübel, T., Emre, Y., Rabier, D., Chadefaux, B., Ricquier, D., and Bouillaud, F. (2008) Modified glutamine catabolism in macrophages of *Ucp2* knock-out mice. *Biochim. Biophys. Acta* **1777**, 48–54 [CrossRef Medline](#)
  39. O'Neill, L. A. J., and Pearce, E. J. (2016) Immunometabolism governs dendritic cell and macrophage function. *J. Exp. Med.* **213**, 15–23 [CrossRef Medline](#)
  40. Ahmadian, M., Suh, J. M., Hah, N., Liddle, C., Atkins, A. R., Downes, M., and Evans, R. M. (2013) PPAR $\gamma$  signaling and metabolism: The good, the bad and the future. *Nat. Med.* **19**, 557–566 [CrossRef Medline](#)
  41. Medvedev, A. V., Snedden, S. K., Raimbault, S., Ricquier, D., and Collins, S. (2001) Transcriptional regulation of the mouse uncoupling protein-2 gene: Double E-box motif is required for peroxisome proliferator-activated receptor- $\gamma$ -dependent activation. *J. Biol. Chem.* **276**, 10817–10823 [CrossRef Medline](#)
  42. Hotamisligil, G. S. (2017) Inflammation, metaflammation and immunometabolic disorders. *Nature* **542**, 177–185 [CrossRef Medline](#)
  43. Kim, J. D., Yoon, N. A., Jin, S., and Diano, S. (2019) Microglial *UCP2* mediates inflammation and obesity induced by high-fat feeding. *Cell Metab.* **30**, 952–962.e5 [CrossRef Medline](#)